Mathematical and Computer Modelling 58 (2013) 379–392

Contents lists available at SciVerse ScienceDirect

Mathematical and Computer Modelling

journal homepage: www.elsevier.com/locate/mcm

Matrix representation of the double-curl operator for simulating three dimensional photonic crystals

Tsung-Ming Huang [a], Han-En Hsieh [b], Wen-Wei Lin [c,*], Weichung Wang [b]

[a] Department of Mathematics, National Taiwan Normal University, Taipei 116, Taiwan

[b] Department of Mathematics, National Taiwan University, Taipei, 106, Taiwan

[c] Department of Applied Mathematics, National Chiao Tung University, Hsinchu 300, Taiwan

ARTICLE INFO

Keywords:
Photonic crystals
Face centered cubic lattice
The Maxwell equations
Yee's scheme
Double-curl operator
Matrix representation

ABSTRACT

Three dimensional photonic crystals can be modeled by the Maxwell equations as a generalized eigenvalue problem (GEVP). Simulations based on the numerical solutions of the GEVP are used to reveal physical properties and boost innovative applications of photonic crystals. However, to solve these GEVP remains a computational challenge in both timing and accuracy. The GEVP corresponding to the photonic crystals with face centered cubic (FCC) lattice is one of the challenging eigenvalue problems. From a viewpoint of matrix computation, we demonstrate how such obstacles can be overcome. Our main contribution is an explicit matrix representation of the double-curl operator associated with the photonic crystal with FCC lattice. This particular matrix represents the degenerate coefficient matrix of the discrete GEVP obtained by Yee's scheme. The explicit matrix leads to an eigendecomposition of the degenerate coefficient matrix and then a fast eigenvalue solver. Promising numerical results in terms of timing and accuracy are reported for solving the discrete GEVP arising in three dimensional photonic crystals with various geometric parameters.

1. Introduction

Photonic crystals are made of space-dependent dielectric materials with periodic structures. Full band gap is the most distinguished feature of photonic crystals and attracts extensive studies in its properties and applications. Numerical simulations play an essential role to predict the band structures of photonic crystals with various geometric settings. Such simulations rely on numerical solutions of the generalized eigenvalue problems (GEVP) that are derived from discretizations of the governing Maxwell equations.

To solve these GEVP, however, is not a trivial task, especially for the three dimensional (3D) photonic crystals. The obstacle is mainly caused by the facts that (i) the desired eigenvalues are located in the interior of the eigenvalue spectrum, (ii) the GEVP are of large size, and (iii) a large null space is associated with the coefficient matrix [1,2]. To find the interior eigenvalues, several eigenvalue solvers have been proposed. The solvers range from the Jacobi–Davidson methods [3–11] to the shift-and-invert type methods, including the inverse power methods [4,12,2,13] and Lanczos/Arnoldi methods [4,6,14]. As the GEVP are large, iterative methods are used to solve the resulting linear systems within the eigenvalue solvers. In addition, to deal with the difficulty due to the null space, several methods have been studied [5,2,9].

* Corresponding author.
E-mail addresses: min@ntnu.edu.tw (T.-M. Huang), d99221002@ntu.edu.tw (H.-E. Hsieh), wwlin@math.nctu.edu.tw (W.-W. Lin), wwang@ntu.edu.tw (W. Wang).

0895-7177/$ – see front matter © 2012 Elsevier Ltd. All rights reserved.
doi:10.1016/j.mcm.2012.11.008

Despite of the different degrees of successes that have been reported in the literature, there is a room to further improve the efficiency of the eigenvalue solvers. In particular, we focus on the GEVP associated with the photonic crystals with the face centered cubic (FCC) lattice. The choice is motivated by the fact that the FCC lattice structure demonstrates larger full band-gap, which is favored in applications in terms of photon localization and photonic defect states. However, it is quite a challenge to develop an efficient method to solve the GEVP associated with the FCC lattice. The corresponding coefficient matrix is very complicated and it is hard to explore the properties of the matrix. To overcome the computational difficulty, an explicit matrix representation of the double-curl operator associated with the 3D FCC photonic crystals is described for the first time in this article. Based on this explicit matrix representation, several matrix properties are revealed and an efficient eigenvalue solver is proposed in [15].

This paper is outlined as follows. We first describe the background material in Section 2. By using Yee's scheme to discretize the Maxwell equations, we derive the degenerate coefficient matrix of the discretized Maxwell equations in Section 3. The resulting matrix property and the eigenvalue solver are then briefly presented in Section 4. Numerical results associated with various geometric parameters are presented in Section 5 to demonstrate the efficiency of the resulting eigenvalue solver. Finally, we conclude the paper in Section 6.

Throughout this paper, we denote the transpose and the conjugate transpose of a matrix by the superscript $\top$ and $*$, respectively. For the matrix operations, we denote $\otimes$ and $\oplus$ the Kronecker product and direct sum of two matrices, respectively. We denote the imaginary number $\sqrt{-1}$ by $\imath$ and the identity matrix of order n by I_n. The conjugate of a complex scalar $z \in \mathbb{C}$ and a complex vector $\mathbf{z} \in \mathbb{C}^n$ are represented by $\bar{z}$ and $\bar{\mathbf{z}}$, respectively. The vec$(\cdot)$ is the operator that vectorizes a matrix by stacking the columns of the matrix.

2. Background

The 3D photonic crystals can be modeled by the Maxwell equations

$$\nabla \times \nabla \times E = \lambda \varepsilon E, \tag{1a}$$

$$\nabla \cdot (\varepsilon E) = 0, \tag{1b}$$

where E is the electric field, $\lambda = \mu_0 \omega^2$ is the unknown eigenvalue, μ_0 is the magnetic constant, ω is the frequency of time, and ε is the material dependent permittivity constants. Since the photonic crystals consist of dielectric materials fabricated in periodic structure, by Bloch's Theorem [16], the electric field E of (1) satisfies the quasi-periodic condition

$$E(\mathbf{x} + \mathbf{a}_\ell) = e^{\imath 2\pi \mathbf{k}\cdot\mathbf{a}_\ell} E(\mathbf{x}), \quad \ell = 1, 2, 3. \tag{2}$$

Here, $2\pi\mathbf{k}$ is the Bloch wave vector in the first Brillouin zone and $\mathbf{a}_\ell$'s are the lattice translation vectors that span the primitive cell which extends periodically to form the photonic crystals. Yee's scheme [17] can be used to discretize the Eq. (1) on a primitive cell with the lattice vectors. The divergence free constraint (1b) is automatically embedded in this approach. The resulting discretized system is a GEVP

$$A\mathbf{e} = \lambda B\mathbf{e}, \tag{3}$$

where A is the degenerate coefficient matrix corresponding to the discrete double-curl operator, $\mathbf{e}$ is the vectorized E in the grid points, and B is a positive diagonal matrix determined by ε.

Now, we discuss the lattice translation vectors and the computational domain related to the GEVP associated with the 3D photonic crystal with face centered cubic (FCC) lattice. The lattice translation vectors of FCC are given as

$$\mathbf{a}_1 = \frac{a}{\sqrt{2}}[1, 0, 0]^\top, \qquad \mathbf{a}_2 = \frac{a}{\sqrt{2}}\left[\frac{1}{2}, \frac{\sqrt{3}}{2}, 0\right]^\top, \qquad \mathbf{a}_3 = \frac{a}{\sqrt{2}}\left[\frac{1}{2}, \frac{1}{2\sqrt{3}}, \sqrt{\frac{2}{3}}\right]^\top, \tag{4}$$

where a is the lattice constant. The length, width, and height of the primitive cell are $\frac{a}{\sqrt{2}}$, $\frac{a\sqrt{3}}{2\sqrt{2}}$ and $\frac{a}{\sqrt{3}}$, respectively. On the other hand, as shown in [18], the standard primitive lattice vectors $\tilde{\mathbf{a}}_1$, $\tilde{\mathbf{a}}_2$, and $\tilde{\mathbf{a}}_3$ for the FCC lattice are

$$\tilde{\mathbb{A}} \equiv \begin{bmatrix}\tilde{\mathbf{a}}_1 & \tilde{\mathbf{a}}_2 & \tilde{\mathbf{a}}_3\end{bmatrix} = \frac{a}{2}\begin{bmatrix}1 & 0 & 1\\ 1 & 1 & 0\\ 0 & 1 & 1\end{bmatrix}.$$

The associated primitive reciprocal lattice vectors $\tilde{\mathbf{b}}_1$, $\tilde{\mathbf{b}}_2$, and $\tilde{\mathbf{b}}_3$ are

$$\begin{bmatrix}\tilde{\mathbf{b}}_1 & \tilde{\mathbf{b}}_2 & \tilde{\mathbf{b}}_3\end{bmatrix} = \frac{2\pi}{a}\begin{bmatrix}1 & -1 & 1\\ 1 & 1 & -1\\ -1 & 1 & 1\end{bmatrix} = 2\pi\begin{bmatrix}\tilde{\mathbf{a}}_1 & \tilde{\mathbf{a}}_2 & \tilde{\mathbf{a}}_3\end{bmatrix}^{-\top}.$$

The corner points of the associated irreducible Brillouin zone are $\tilde{X} = \frac{2\pi}{a}(0, 1, 0)$, $\tilde{U} = \frac{2\pi}{a}(\frac{1}{4}, 1, \frac{1}{4})$, $\tilde{L} = \frac{2\pi}{a}(\frac{1}{2}, \frac{1}{2}, \frac{1}{2})$, $\tilde{\Gamma} = (0, 0, 0)$, $\tilde{W} = \frac{2\pi}{a}(\frac{1}{2}, 1, 0)$, and $\tilde{K} = \frac{2\pi}{a}(\frac{3}{4}, \frac{3}{4}, 0)$. Consequently, for the new primitive lattice vectors $\mathbf{a}_1$, $\mathbf{a}_2$, and $\mathbf{a}_3$ in (4), the associated primitive reciprocal lattice vectors $\mathbf{b}_1$, $\mathbf{b}_2$, and $\mathbf{b}_3$ are given as

$$\begin{bmatrix}\mathbf{b}_1 & \mathbf{b}_2 & \mathbf{b}_3\end{bmatrix} = 2\pi\begin{bmatrix}\mathbf{a}_1 & \mathbf{a}_2 & \mathbf{a}_3\end{bmatrix}^{-\top}.$$

Since $\begin{bmatrix}\mathbf{b}_1 & \mathbf{b}_2 & \mathbf{b}_3\end{bmatrix}$ and $\begin{bmatrix}\tilde{\mathbf{b}}_1 & \tilde{\mathbf{b}}_2 & \tilde{\mathbf{b}}_3\end{bmatrix}$ satisfy the relation

$$\begin{bmatrix}\mathbf{b}_1 & \mathbf{b}_2 & \mathbf{b}_3\end{bmatrix} = Q\begin{bmatrix}\tilde{\mathbf{b}}_1 & \tilde{\mathbf{b}}_2 & \tilde{\mathbf{b}}_3\end{bmatrix},$$

where

$$\begin{aligned} Q &= \begin{bmatrix}\mathbf{b}_1 & \mathbf{b}_2 & \mathbf{b}_3\end{bmatrix}\begin{bmatrix}\tilde{\mathbf{b}}_1 & \tilde{\mathbf{b}}_2 & \tilde{\mathbf{b}}_3\end{bmatrix}^{-1} = \begin{bmatrix}\mathbf{a}_1 & \mathbf{a}_2 & \mathbf{a}_3\end{bmatrix}^{-\top}\begin{bmatrix}\tilde{\mathbf{a}}_1 & \tilde{\mathbf{a}}_2 & \tilde{\mathbf{a}}_3\end{bmatrix}^{\top} \\ &= \frac{\sqrt{2}}{a}\begin{bmatrix} 1 & 0 & 0 \\ -\frac{1}{\sqrt{3}} & \frac{2}{\sqrt{3}} & 0 \\ -\frac{1}{\sqrt{6}} & -\frac{1}{\sqrt{6}} & \sqrt{\frac{3}{2}} \end{bmatrix}\frac{a}{2}\begin{bmatrix}1 & 1 & 0\\ 0 & 1 & 1\\ 1 & 0 & 1\end{bmatrix} = \frac{1}{\sqrt{2}}\begin{bmatrix} 1 & 1 & 0 \\ -\frac{1}{\sqrt{3}} & \frac{1}{\sqrt{3}} & \frac{2}{\sqrt{3}} \\ \frac{2}{\sqrt{6}} & -\frac{2}{\sqrt{6}} & \frac{2}{\sqrt{6}} \end{bmatrix}. \end{aligned}$$

We define the new corner points of the new irreducible Brillouin zone for primitive lattice vectors $\mathbf{a}_1$, $\mathbf{a}_2$, and $\mathbf{a}_3$ by $X = Q\tilde{X}$, $U = Q\tilde{U}$, $L = Q\tilde{L}$, $\Gamma = \tilde{\Gamma}$, $W = Q\tilde{W}$, and $K = Q\tilde{K}$. It is worth noting that the band structure can be computed by solving the eigenvalue problems associated with the $\mathbf{k}$'s along the segments connecting X, U, L, Γ, X, W, and K.

3. Explicit matrix representation of the double-curl operator

We use Yee's scheme [17] to discretize Eq. (1) and derive the explicit matrix representation form of the corresponding operators to form the GEVP (3) explicitly. Letting

$$H = \nabla \times E, \tag{5}$$

we have

$$\nabla \times H = \lambda\varepsilon E \tag{6}$$

from (1). Based on this observation, the matrix representation is derived in two stages: (i) the matrix form of $H = \nabla \times E$ is first derived in Section 3.1 and (ii) the matrix form of $\nabla \times H = \lambda\varepsilon E$ is derived in Section 3.2.

We use the following notations in our derivations. Denoting $E = [E_1, E_2, E_3]^\top$, $H = [H_1, H_2, H_3]^\top$, and $\varepsilon = [\varepsilon_1, \varepsilon_2, \varepsilon_3]^\top$, Eqs. (5) and (6) can be rewritten as

$$\begin{cases} \partial_y E_3 - \partial_z E_2 = H_1, \\ \partial_z E_1 - \partial_x E_3 = H_2, \\ \partial_x E_2 - \partial_y E_1 = H_3, \end{cases} \tag{7}$$

and

$$\begin{cases} \partial_y H_3 - \partial_z H_2 = \lambda\varepsilon E_1, \\ \partial_z H_1 - \partial_x H_3 = \lambda\varepsilon E_2, \\ \partial_x H_2 - \partial_y H_1 = \lambda\varepsilon E_3, \end{cases} \tag{8}$$

respectively. Note that Eqs. (7) and (8) are discretized at the centers of cell faces and edges, respectively, in Yee's scheme.

In the partitions, the constants δ_x, δ_y, and δ_z denote the grid length along the x, y, and z axial directions, respectively. The constants n_1, n_2, and n_3 are the numbers of grid points in x, y, and z directions, respectively, and $n = n_1 n_2 n_3$. We further assume that $n_1 = 6m_1$, $n_2 = 6m_2$, and $n_3 = 6m_3$ to assure n_1, n_2, and n_3 are multiples of six.

The approximate function values due to finite differences are represented by the grid points indexed by i, j, and k and the "half grid points" indexed by $\hat{i} = i + \frac{1}{2}$, $\hat{j} = j + \frac{1}{2}$, and $\hat{k} = k + \frac{1}{2}$. For simplicity, we represent an arbitrary point $(r\delta_x, s\delta_y, t\delta_z)$ in the computational domain by $\mathbf{x}(r, s, t)$, where $r, s, t \in \mathbb{R}$. That is,

$$\mathbf{x}(r, s, t) = (r\delta_x, s\delta_y, t\delta_z). \tag{9}$$

For $i = 0, \ldots, n_1 - 1$, $j = 0, \ldots, n_2 - 1$, and $k = 0, \ldots, n_3 - 1$, we define the following notations.

- Let $E_1(\hat{i}, j, k)$, $E_2(i, \hat{j}, k)$, and $E_3(i, j, \hat{k})$ denote approximate values of functions E_1, E_2, and E_3 in vector forms, at the central edge points $\mathbf{x}(\hat{i}, j, k)$, $\mathbf{x}(i, \hat{j}, k)$, and $\mathbf{x}(i, j, \hat{k})$, respectively.
- Let $H_1(i, \hat{j}, \hat{k})$, $H_2(\hat{i}, j, \hat{k})$, and $H_3(\hat{i}, \hat{j}, k)$ denote approximate values of functions H_1, H_2, and H_3 in vector forms at the central face points $\mathbf{x}(i, \hat{j}, \hat{k})$, $\mathbf{x}(\hat{i}, j, \hat{k})$, and $\mathbf{x}(\hat{i}, \hat{j}, k)$, respectively.
- Set $B_1(\hat{i}, j, k) = \varepsilon_1(\mathbf{x}(\hat{i}, j, k))$, $B_2(i, \hat{j}, k) = \varepsilon_2(\mathbf{x}(i, \hat{j}, k))$, and $B_3(i, j, \hat{k}) = \varepsilon_3(\mathbf{x}(i, j, \hat{k}))$.

Finally, by using the vectorization function of a matrix $F \in \mathbb{C}^{m_1 \times m_2 \times m_3}$ that

$$\operatorname{vec}(F) = \begin{bmatrix} \operatorname{vec}(F(1 : m_1, 1 : m_2, 1)) \\ \operatorname{vec}(F(1 : m_1, 1 : m_2, 2)) \\ \vdots \\ \operatorname{vec}(F(1 : m_1, 1 : m_2, m_3)) \end{bmatrix},$$

we define

$$\mathbf{e} = \begin{bmatrix}\mathbf{e}_1^\top & \mathbf{e}_2^\top & \mathbf{e}_3^\top\end{bmatrix}^\top \in \mathbb{C}^{3n} \tag{10}$$

and

$$\mathbf{h} = \begin{bmatrix}\mathbf{h}_1^\top & \mathbf{h}_2^\top & \mathbf{h}_3^\top\end{bmatrix}^\top \in \mathbb{C}^{3n},$$

with $\mathbf{e}_\ell = \mathrm{vec}(E_\ell)$ and $\mathbf{h}_\ell = \mathrm{vec}(H_\ell)$, for $\ell = 1, 2, 3$. We define the $3n$-by-$3n$ diagonal matrix

$$B = \mathrm{diag}\left[\begin{bmatrix}\mathrm{vec}(B_1)^\top, \mathrm{vec}(B_2)^\top, \mathrm{vec}(B_3)^\top\end{bmatrix}^\top\right] \in \mathbb{C}^{3n\times 3n}.$$

3.1. Matrix representation of $H = \nabla \times E$

In this subsection, we derive the matrix representation of the discretization for (7) by finite differences at the central face points $\mathbf{x}(i, \hat{j}, \hat{k})$, $\mathbf{x}(\hat{i}, j, \hat{k})$, and $\mathbf{x}(\hat{i}, \hat{j}, k)$, respectively. As we will show in the theorems, the key point is to explore the periodic properties associated with the lattice translation vectors that define the structure of the target photonic crystals.

The matrix representation derivation of the single curl $\nabla \times (\cdot)$ involves the partial derivatives. We separate the discretization of the partial derivatives with respect to x, y, and z in the following three parts, with a short summary.

Part I. Partial derivative with respect to x for E. Consider the finite difference discretization of $\partial_x E_2$ at $\mathbf{x}(\hat{i}, \hat{j}, k)$ and $\partial_x E_3$ at $\mathbf{x}(\hat{i}, j, \hat{k})$ that are written as

$$\frac{E_2(i+1, \hat{j}, k) - E_2(i, \hat{j}, k)}{\delta_x} \quad \text{and} \quad \frac{E_3(i+1, j, \hat{k}) - E_3(i, j, \hat{k})}{\delta_x}, \tag{11}$$

respectively, for $i = 0, 1, \ldots, n_1 - 1$, $j = 0, 1, \ldots, n_2 - 1$, and $k = 0, 1, \ldots, n_3 - 1$. By Theorem 1 shown below and the notation $\mathbf{e}_\ell$ defined in (10), the matrix representations of the discretizations in (11) are $C_1\mathbf{e}_2$ and $C_1\mathbf{e}_3$, respectively. Here,

$$C_1 = I_{n_2\times n_3} \otimes K_1 \in \mathbb{C}^{n\times n}$$

and

$$K_1 = \frac{1}{\delta_x}\begin{bmatrix} -1 & 1 & & \\ & \ddots & \ddots & \\ & & -1 & 1 \\ e^{\imath 2\pi \mathbf{k}\cdot\mathbf{a}_1} & & & -1 \end{bmatrix} \in \mathbb{C}^{n_1\times n_1}.$$

Theorem 1 (*Periodicity along $\mathbf{a}_1$*). *Applying the periodic condition (2) along the lattice translation vector $\mathbf{a}_1$ defined in (4), we have*

$$E_2(n_1, \hat{j}, k) = e^{\imath 2\pi \mathbf{k}\cdot\mathbf{a}_1} E_2(0, \hat{j}, k) \quad \textit{and} \quad E_3(n_1, j, \hat{k}) = e^{\imath 2\pi \mathbf{k}\cdot\mathbf{a}_1} E_3(0, j, \hat{k}),$$

for $j = 0, 1, \ldots, n_2 - 1$ and $k = 0, 1, \ldots, n_3 - 1$.

Proof. The proof is straightforward by the periodic condition (2). □

Part II. Partial derivative with respect to y for E. Consider the finite difference discretization of $\partial_y E_1$ at $\mathbf{x}(\hat{i}, \hat{j}, k)$ and $\partial_y E_3$ at $\mathbf{x}(i, \hat{j}, \hat{k})$ that are written as

$$\frac{E_1(\hat{i}, j+1, k) - E_1(\hat{i}, j, k)}{\delta_y} \quad \text{and} \quad \frac{E_3(i, j+1, \hat{k}) - E_3(i, j, \hat{k})}{\delta_y}, \tag{12}$$

respectively, for $i = 0, 1, \ldots, n_1 - 1$, $j = 0, 1, \ldots, n_2 - 1$, and $k = 0, 1, \ldots, n_3 - 1$. By Theorem 2 shown below, the discretizations in (12) can be represented as

$$K_2\mathrm{vec}(E_1(\hat{0} : \hat{n}_1 - 1, 0 : n_2 - 1, k)) \quad \text{and} \quad K_2\mathrm{vec}(E_3(0 : n_1 - 1, 0 : n_2 - 1, \hat{k})),$$

respectively, for $k = 0, 1, \ldots, n_3 - 1$ and

$$K_2 = \frac{1}{\delta_y}\begin{bmatrix} -I_{n_1} & I_{n_1} & & \\ & \ddots & \ddots & \\ & & -I_{n_1} & I_{n_1} \\ e^{\imath 2\pi \mathbf{k}\cdot\mathbf{a}_2} J_2 & & & -I_{n_1} \end{bmatrix} \in \mathbb{C}^{(n_1 n_2)\times(n_1 n_2)}.$$

Or equivalently, the matrix representations of the discretizations in (12) are $C_2\mathbf{e}_1$ and $C_2\mathbf{e}_3$, respectively. Here,

$$C_2 = I_{n_3} \otimes K_2 \in \mathbb{C}^{n\times n}.$$

Theorem 2 (*Periodicity along* $\mathbf{a}_1$ *and* $\mathbf{a}_2$)**.** *Applying the quasi-periodic condition* (2) *along the lattice translation vectors* $\mathbf{a}_1$ *and* $\mathbf{a}_2$ *defined in* (4)*, we have*

$$E_1(\hat{0} : \hat{n}_1 - 1, n_2, k) = e^{\imath 2\pi \mathbf{k}\cdot\mathbf{a}_2} J_2 E_1(\hat{0} : \hat{n}_1 - 1, 0, k) \tag{13}$$

and

$$E_3(0 : n_1 - 1, n_2, \hat{k}) = e^{\imath 2\pi \mathbf{k}\cdot\mathbf{a}_2} J_2 E_3(0 : n_1 - 1, 0, \hat{k}), \tag{14}$$

where

$$J_2 = \begin{bmatrix} 0 & e^{-\imath 2\pi \mathbf{k}\cdot\mathbf{a}_1} I_{\frac{1}{2}n_1} \\ I_{\frac{1}{2}n_1} & 0 \end{bmatrix} \in \mathbb{C}^{n_1 \times n_1}.$$

Proof. By the definitions in (9), we have

$$\mathbf{x}(i, n_2, \hat{k}) = \mathbf{a}_2 + \left(\frac{i - 3m_1}{6m_1} \frac{a}{\sqrt{2}}, 0, \hat{k}\delta_z \right). \tag{15}$$

If $0 \le i < 3m_1$, the vector in (15) can be rewritten as

$$\mathbf{x}(i, n_2, \hat{k}) = \mathbf{a}_2 - \mathbf{a}_1 + \left(\frac{3m_1 + i}{6m_1} \frac{a}{\sqrt{2}}, 0, \hat{k}\delta_z \right) = \mathbf{a}_2 - \mathbf{a}_1 + \mathbf{x}(3m_1 + i, 0, \hat{k});$$

otherwise, we have

$$\mathbf{x}(i, n_2, \hat{k}) = \mathbf{a}_2 + \mathbf{x}(i - 3m_1, 0, \hat{k}).$$

The above rewritten implies that

$$E_3(i, n_2, \hat{k}) = \begin{cases} e^{\imath 2\pi \mathbf{k}\cdot(\mathbf{a}_2 - \mathbf{a}_1)} E_3(3m_1 + i, 0, \hat{k}), & \text{if } 0 \le i < 3m_1, \\ e^{\imath 2\pi \mathbf{k}\cdot\mathbf{a}_2} E_3(i - 3m_1, 0, \hat{k}), & \text{if } 3m_1 \le i \le 6m_1 - 1. \end{cases} \tag{16a}$$

Similarly,

$$E_1(\hat{i}, n_2, k) = \begin{cases} e^{\imath 2\pi \mathbf{k}\cdot(\mathbf{a}_2 - \mathbf{a}_1)} E_1(3m_1 + \hat{i}, 0, k), & \text{if } 0 \le i < 3m_1, \\ e^{\imath 2\pi \mathbf{k}\cdot\mathbf{a}_2} E_1(\hat{i} - 3m_1, 0, k), & \text{if } 3m_1 \le i \le 6m_1 - 1. \end{cases} \tag{16b}$$

The results in (13) and (14) can then be obtained by substituting i from 0 to $n_1 - 1$ into (16). □

Part III. Partial derivative with respect to z **for** E. Consider the finite difference discretization of $\partial_z E_1$ at $\mathbf{x}(\hat{i}, j, \hat{k})$ and $\partial_z E_2$ at $\mathbf{x}(i, \hat{j}, \hat{k})$ that are written as

$$\frac{E_1(\hat{i}, j, k+1) - E_1(\hat{i}, j, k)}{\delta_z} \quad \text{and} \quad \frac{E_2(i, \hat{j}, k+1) - E_2(i, \hat{j}, k)}{\delta_z}, \tag{17}$$

respectively, for $i = 0, 1, \ldots, n_1 - 1$, $j = 0, 1, \ldots, n_2 - 1$, and $k = 0, 1, \ldots, n_3 - 1$. By Theorem 3 shown below, the matrix representations of the discretizations in (17) are $C_3\mathbf{e}_1$ and $C_3\mathbf{e}_2$, respectively. Here,

$$C_3 \equiv K_3 = \frac{1}{\delta_z} \begin{bmatrix} -I_{n_1 \times n_2} & I_{n_1 \times n_2} & & \\ & \ddots & \ddots & \\ & & -I_{n_1 \times n_2} & I_{n_1 \times n_2} \\ e^{\imath 2\pi \mathbf{k}\cdot\mathbf{a}_3} J_3 & & & -I_{n_1 \times n_2} \end{bmatrix} \in \mathbb{C}^{n \times n}.$$

Theorem 3 (*Periodicity along* $\mathbf{a}_1$, $\mathbf{a}_2$, *and* $\mathbf{a}_3$)**.** *Applying the quasi-periodic condition* (2) *along the lattice translation vectors* $\mathbf{a}_1$, $\mathbf{a}_2$, *and* $\mathbf{a}_3$ *defined in* (4)*, we have*

$$\mathrm{vec}(E_1(\hat{0} : \hat{n}_1 - 1, 0 : n_2 - 1, n_3)) = e^{\imath 2\pi \mathbf{k}\cdot\mathbf{a}_3} J_3 \mathrm{vec}(E_1(\hat{0} : \hat{n}_1 - 1, 0 : n_2 - 1, 0)) \tag{18}$$

and

$$\mathrm{vec}(E_2(0 : n_1 - 1, \hat{0} : \hat{n}_2 - 1, n_3)) = e^{\imath 2\pi \mathbf{k}\cdot\mathbf{a}_3} J_3 \mathrm{vec}(E_2(0 : n_1 - 1, \hat{0} : \hat{n}_2 - 1, 0)), \tag{19}$$

where

$$J_3 = \begin{bmatrix} 0 & e^{-\imath 2\pi \mathbf{k}\cdot\mathbf{a}_2} I_{\frac{1}{3}n_2} \otimes I_{n_1} \\ I_{\frac{2}{3}n_2} \otimes J_2 & 0 \end{bmatrix} \in \mathbb{C}^{(n_1 n_2) \times (n_1 n_2)}.$$

Proof. Observing

$$\mathbf{x}(i,\hat{j},n_3)=\mathbf{a}_3+\left(\frac{i-3m_1}{6m_1}\frac{a}{\sqrt{2}},\frac{j+1/2-2m_2}{6m_2}\frac{\sqrt{3}a}{2\sqrt{2}},0\right),$$

we have the following results. If $0\le j<2m_2$, then

$$\begin{aligned}\mathbf{x}(i,\hat{j},n_3)&=\mathbf{a}_3-\mathbf{a}_2+\left(\frac{i}{6m_1}\frac{a}{\sqrt{2}},\frac{j+1/2+4m_2}{6m_2}\frac{\sqrt{3}a}{2\sqrt{2}},0\right)\\&=\mathbf{a}_3-\mathbf{a}_2+\mathbf{x}(i,4m_2+\hat{j},0).\end{aligned}$$

If $2m_2\le j<6m_2$ and $0\le i<3m_1$, then

$$\begin{aligned}\mathbf{x}(i,\hat{j},n_3)&=\mathbf{a}_3-\mathbf{a}_1+\left(\frac{i+3m_1}{6m_1}\frac{a}{\sqrt{2}},\frac{j+1/2-2m_2}{6m_2}\frac{\sqrt{3}a}{2\sqrt{2}},0\right)\\&=\mathbf{a}_3-\mathbf{a}_1+\mathbf{x}(3m_1+i,\hat{j}-2m_2,0).\end{aligned}$$

In other cases, i.e., $2m_2\le j<6m_2$ and $3m_1\le i<6m_1$,

$$\mathbf{x}(i,\hat{j},n_3)=\mathbf{a}_3+\mathbf{x}(i-3m_1,\hat{j}-2m_2,0).$$

Consequently, $E_2(i,\hat{j},n_3)$ can be rewritten as

$$E_2(i,\hat{j},n_3)=\begin{cases}e^{i2\pi\mathbf{k}\cdot(\mathbf{a}_3-\mathbf{a}_2)}E_2(i,4m_2+\hat{j},0), & \text{if } 0\le j<2m_2,\\ e^{i2\pi\mathbf{k}\cdot(\mathbf{a}_3-\mathbf{a}_1)}E_2(3m_1+i,\hat{j}-2m_2,0), & \text{if } 2m_2\le j<6m_2,\ 0\le i<3m_1,\\ e^{i2\pi\mathbf{k}\cdot\mathbf{a}_3}E_2(i-3m_1,\hat{j}-2m_2,0), & \text{if } 2m_2\le j<6m_2,\ 3m_1\le i<6m_1.\end{cases}\tag{20}$$

Using (20) with $i=0,1,\ldots,n_1-1$ and $j=0,1,\ldots,n_2-1$, we prove the periodicity shown in (19). The periodicity shown in (18) can be obtained similarly. □

A short summary. We have shown that the discretization of $H=\nabla\times E$ at central face points can be represented by the following matrix representation

$$\mathbf{h}=C\mathbf{e},\tag{21}$$

where

$$C=\begin{bmatrix}0 & -C_3 & C_2\\ C_3 & 0 & -C_1\\ -C_2 & C_1 & 0\end{bmatrix}.$$

3.2. Matrix representation of $\nabla\times H=\lambda\varepsilon E$

Now, we derive the matrix representation for the three equations in (8) by central finite differences at the central edge points $\mathbf{x}(\hat{i},j,k)$, $\mathbf{x}(i,\hat{j},k)$, and $\mathbf{x}(i,j,\hat{k})$, respectively. First, we define the following notations based on the discretization of $H=\nabla\times E$:

$$H_1(i,\hat{j},\hat{k})=\frac{E_3(i,j+1,\hat{k})-E_3(i,j,\hat{k})}{\delta_y}-\frac{E_2(i,\hat{j},k+1)-E_2(i,\hat{j},k)}{\delta_z},\tag{22a}$$

$$H_2(\hat{i},j,\hat{k})=\frac{E_1(\hat{i},j,k+1)-E_1(\hat{i},j,k)}{\delta_z}-\frac{E_3(i+1,j,\hat{k})-E_3(i,j,\hat{k})}{\delta_x},\tag{22b}$$

$$H_3(\hat{i},\hat{j},k)=\frac{E_2(i+1,\hat{j},k)-E_2(i,\hat{j},k)}{\delta_x}-\frac{E_1(\hat{i},j+1,k)-E_1(\hat{i},j,k)}{\delta_y},\tag{22c}$$

for $i=0,1,\ldots,n_1-1$, $j=0,1,\ldots,n_2-1$, and $k=0,1,\ldots,n_3-1$. The notations in Eq. (22) are useful for analyzing the periodic properties of H_ℓ. These periodical properties are analyzed in Theorems 4–6 shown below. The proofs of these theorems are given in the Appendix. The matrix representation of $\nabla\times H$ are then derived in the following three parts. A short summary is then presented to illustrate the matrix representation of $\nabla\times H=\lambda\varepsilon E$.

Part IV. Partial derivative with respect to x for H. Consider the finite difference discretization of $\partial_x H_2$ at $\mathbf{x}(i, j, \hat{k})$ and $\partial_x H_3$ at $\mathbf{x}(i, \hat{j}, k)$ that are written as

$$\frac{H_2(\hat{i}, j, \hat{k}) - H_2(\hat{i}-1, j, \hat{k})}{\delta_x} \quad \text{and} \quad \frac{H_3(\hat{i}, \hat{j}, k) - H_3(\hat{i}-1, \hat{j}, k)}{\delta_x}, \tag{23}$$

for $i = 0, \ldots, n_1 - 1$, $j = 0, \ldots, n_2 - 1$, and $k = 0, \ldots, n_3 - 1$. By Theorem 4 shown below, the matrix representations of the discretizations in (23) are $-C_1^*\mathbf{h}_2$ and $-C_1^*\mathbf{h}_3$.

Theorem 4 (*Periodicity of $H_2(\hat{i}, j, \hat{k})$ and $H_3(\hat{i}, \hat{j}, k)$*). *By (22b), (22c), and the periodicity of E_ℓ, for $\ell = 1, 2, 3$, we have*

$$H_2(\widehat{-1}, j, \hat{k}) = e^{-\imath 2\pi \mathbf{k}\cdot\mathbf{a}_1} H_2(\hat{n}_1, j, \hat{k}) \quad \text{and} \quad H_3(\widehat{-1}, \hat{j}, k) = e^{-\imath 2\pi \mathbf{k}\cdot\mathbf{a}_1} H_3(\hat{n}_1, \hat{j}, k),$$

for $j = 0, 1, \ldots, n_2 - 1$ and $k = 0, 1, \ldots, n_3 - 1$.

Part V. Partial derivative with respect to y for H. Consider the finite difference discretization of $\partial_y H_1$ at $\mathbf{x}(i, j, \hat{k})$ and $\partial_y H_3$ at $\mathbf{x}(\hat{i}, j, k)$ that are written as

$$\frac{H_1(i, \hat{j}, \hat{k}) - H_1(i, \hat{j}-1, \hat{k})}{\delta_y} \quad \text{and} \quad \frac{H_3(\hat{i}, \hat{j}, k) - H_3(\hat{i}, \hat{j}-1, k)}{\delta_y}, \tag{24}$$

for $i = 0, 1, \ldots, n_1 - 1$, $j = 0, 1, \ldots, n_2 - 1$, and $k = 0, 1, \ldots, n_3 - 1$. By Theorem 5 shown below, the matrix representations of the discretizations in (24) are $-K_2^*\mathrm{vec}(H_1(0 : n_1 - 1, \hat{0} : \hat{n}_2 - 1, \hat{k}))$ and $-K_2^*\mathrm{vec}(H_3(\hat{0} : \hat{n}_1 - 1, \hat{0} : \hat{n}_2 - 1, k))$, for $k = 0, 1, \ldots, n_3 - 1$. In other words, the matrix representation of the discretizations for $\partial_y H_1$ and $\partial_y H_3$ are $-C_2^*\mathbf{h}_1$ and $-C_2^*\mathbf{h}_3$, respectively.

Theorem 5 (*Periodicity of $H_1(i, \hat{j}, \hat{k})$ and $H_3(\hat{i}, \hat{j}, k)$*). *By (22a), (22c), and the periodicity of E_ℓ, for $\ell = 1, 2, 3$, we have*

$$H_1(0 : n_1 - 1, \widehat{-1}, \hat{k}) = e^{-\imath 2\pi \mathbf{k}\cdot\mathbf{a}_2} J_2^* H_1(0 : n_1 - 1, \hat{n}_2 - 1, \hat{k}) \quad \text{and}$$
$$H_3(\hat{0} : \hat{n}_1 - 1, \widehat{-1}, k) = e^{-\imath 2\pi \mathbf{k}\cdot\mathbf{a}_2} J_2^* H_3(\hat{0} : \hat{n}_1 - 1, \hat{n}_2 - 1, k),$$

for $k = 0, 1, \ldots, n_3 - 1$.

Part VI. Partial derivative with respect to z for H. Consider the finite difference discretization of $\partial_z H_1$ at $\mathbf{x}(i, \hat{j}, k)$ and $\partial_z H_2$ at $\mathbf{x}(\hat{i}, j, k)$ that are written as

$$\frac{H_1(i, \hat{j}, \hat{k}) - H_1(i, \hat{j}, \hat{k}-1)}{\delta_z} \quad \text{and} \quad \frac{H_2(\hat{i}, j, \hat{k}) - H_2(\hat{i}, j, \hat{k}-1)}{\delta_z}, \tag{25}$$

for $i = 0, 1, \ldots, n_1 - 1$, $j = 0, 1, \ldots, n_2 - 1$, and $k = 0, 1, \ldots, n_3 - 1$. By Theorem 6 shown below, the matrix representations of the discretizations in (25) are $-C_3^*\mathbf{h}_1$ and $-C_3^*\mathbf{h}_2$.

Theorem 6 (*Periodicity of $H_1(i, \hat{j}, \hat{k})$ and $H_2(\hat{i}, j, \hat{k})$*). *By (22a), (22b), and the periodicity of E_ℓ, for $\ell = 1, 2, 3$, we have*

$$\mathrm{vec}\left(H_1(0 : n_1 - 1, \hat{0} : \hat{n}_2 - 1, \widehat{-1})\right) = e^{-\imath 2\pi \mathbf{k}\cdot\mathbf{a}_3} J_3^* \mathrm{vec}\left(H_1(0 : n_1 - 1, \hat{0} : \hat{n}_2 - 1, \hat{n}_3 - 1)\right) \quad \text{and} \tag{26}$$

$$\mathrm{vec}\left(H_2(\hat{0} : \hat{n}_1 - 1, 0 : n_2 - 1, \widehat{-1})\right) = e^{-\imath 2\pi \mathbf{k}\cdot\mathbf{a}_3} J_3^* \mathrm{vec}\left(H_2(\hat{0} : \hat{n}_1 - 1, 0 : n_2 - 1, \hat{n}_3 - 1)\right). \tag{27}$$

A summary. Combining the aforementioned results, the discretization of $\nabla \times H = \lambda \varepsilon E$ can be represented by the following matrix representation

$$C^*\mathbf{h} = \lambda B\mathbf{e}. \tag{28}$$

Furthermore, by substituting (21) into (28), the discretization of (1) at edges forms the following target GEVP

$$A\mathbf{e} = \lambda B\mathbf{e}, \tag{29}$$

where

$$A = C^*C. \tag{30}$$

Finally, by letting $G = \begin{bmatrix} C_1^\top & C_2^\top & C_3^\top \end{bmatrix}^\top$, we conclude this section by the following remarks.

(i) Comparing the results in Theorems 1–3 with Theorems 4–6, we see that (E_1, E_2, E_3) and (H_1, H_2, H_3) have the same periodic properties.
(ii) The matrices C_1, C_2, and C_3 are the discretizations of the operators ∂_x, ∂_y and ∂_z at the central face points, respectively.
(iii) $C_1^\star$, $C_2^\star$ and $C_3^\star$ are the discretizations of the operators $-\partial_x$, $-\partial_y$ and $-\partial_z$, at the central edge points, respectively.
(iv) The matrices C^*C and $I_3 \otimes (G^*G)$ are the discretizations of the operators $\nabla \times \nabla \times$ and $-\nabla^2$ at the central edge points, respectively.
(v) The matrix GG^* is the discretization of the operator $-\nabla(\nabla\cdot)$ at the central edge points.

4. Eigendecompositions and the fast eigenvalue solver

The explicit matrix representation of the Maxwell equations derived in Section 3 is applied to derive the eigendecomposition of the matrix A in [15]. First, define

$$\theta_i = \frac{\imath 2\pi i}{n_1} + \frac{\imath 2\pi \mathbf{k}\cdot\mathbf{a}_1}{n_1},$$
$$\theta_{i,j} = \frac{\imath 2\pi j}{n_2} + \frac{\imath 2\pi}{n_2}\left\{\mathbf{k}\cdot\hat{\mathbf{a}}_2 - \frac{i}{2}\right\},$$
$$\theta_{i,j,k} = \frac{\imath 2\pi k}{n_3} + \frac{\imath 2\pi}{n_3}\left\{\mathbf{k}\cdot\hat{\mathbf{a}}_3 - \frac{1}{3}(i+j)\right\},$$

and

$$\mathbf{x}_i = \begin{bmatrix}1 & e^{\theta_i} & e^{2\theta_i} & \cdots & e^{(n_1-1)\theta_i}\end{bmatrix}^\top,$$
$$\mathbf{y}_{i,j} = \begin{bmatrix}1 & e^{\theta_{i,j}} & e^{2\theta_{i,j}} & \cdots & e^{(n_2-1)\theta_{i,j}}\end{bmatrix}^\top,$$
$$\mathbf{z}_{i,j,k} = \begin{bmatrix}1 & e^{\theta_{i,j,k}} & e^{2\theta_{i,j,k}} & \cdots & e^{(n_3-1)\theta_{i,j,k}}\end{bmatrix}^\top$$

for $i = 1,\ldots,n_1$, $j = 1,\ldots,n_2$, and $k = 1,\ldots,n_3$. Furthermore, we define

$$\Lambda_q = \Lambda_{\mathbf{x}}^*\Lambda_{\mathbf{x}} + \Lambda_{\mathbf{y}}^*\Lambda_{\mathbf{y}} + \Lambda_{\mathbf{z}}^*\Lambda_{\mathbf{z}} \quad \text{and} \tag{31}$$
$$\Lambda_p = (\Lambda_{\mathbf{x}} + \Lambda_{\mathbf{y}} + \Lambda_{\mathbf{z}})(\Lambda_{\mathbf{x}} + \Lambda_{\mathbf{y}} + \Lambda_{\mathbf{z}})^* \equiv \Lambda_s\Lambda_s^*, \tag{32}$$

where

$$\Lambda_{\mathbf{x}} = \Lambda_{n_1}\otimes I_{n_2n_3}, \qquad \Lambda_{\mathbf{y}} = \left(\oplus_{i=1}^{n_1}\Lambda_{i,n_2}\right)\otimes I_{n_3}, \qquad \Lambda_{\mathbf{z}} = \oplus_{i=1}^{n_1}\oplus_{j=1}^{n_2}\Lambda_{i,j,n_3}, \tag{33}$$

with

$$\Lambda_{n_1} = \delta_x^{-1}\mathrm{diag}\left(e^{\theta_1}-1, e^{\theta_2}-1,\ldots,e^{\theta_{n_1}}-1\right),$$
$$\Lambda_{i,n_2} = \delta_y^{-1}\mathrm{diag}\left(e^{\theta_{i,1}}-1, e^{\theta_{i,2}}-1,\ldots,e^{\theta_{i,n_2}}-1\right),$$
$$\Lambda_{i,j,n_3} = \delta_z^{-1}\mathrm{diag}\left(e^{\theta_{i,j,1}}-1, e^{\theta_{i,j,2}}-1,\ldots,e^{\theta_{i,j,n_3}}-1\right).$$

We define the unitary matrix T as

$$T = \frac{1}{\sqrt{n_1n_2n_3}}\begin{bmatrix}T_1 & T_2 & \cdots & T_{n_1}\end{bmatrix} \in \mathbb{C}^{n\times n} \tag{34}$$

with $T_i = \begin{bmatrix}T_{i,1} & T_{i,2} & \cdots & T_{i,n_2}\end{bmatrix} \in \mathbb{C}^{n\times(n_2n_3)}$ and

$$T_{i,j} = \begin{bmatrix}\mathbf{z}_{i,j,1}\otimes\mathbf{y}_{i,j}\otimes\mathbf{x}_i & \mathbf{z}_{i,j,2}\otimes\mathbf{y}_{i,j}\otimes\mathbf{x}_i & \cdots & \mathbf{z}_{i,j,n_3}\otimes\mathbf{y}_{i,j}\otimes\mathbf{x}_i\end{bmatrix} \in \mathbb{C}^{n\times n_3}$$

for $i = 1,\ldots,n_1$ and $j = 1,\ldots,n_2$.

In addition, by defining a set $\mathcal{B}$ for Bloch wave vectors associated with lattice vectors in (4) by

$$\mathcal{B} = \left\{\mathbf{k} = (\mathrm{k}_1,\mathrm{k}_2,\mathrm{k}_3)^\top \neq \mathbf{0} \,\middle|\, 0\le \mathrm{k}_1 \le \frac{\sqrt{2}}{a}, 0\le \mathrm{k}_2 < \frac{2\sqrt{2}}{\sqrt{3}a}, 0\le \mathrm{k}_3 < \frac{\sqrt{3}}{a}, \text{ and } \mathbf{k}\neq\frac{\sqrt{2}}{a}\left[1,\frac{1}{\sqrt{3}},\frac{1}{\sqrt{6}}\right]^\top\right\},$$

we have Λ_q is positive definite for $\mathbf{k}\in\mathcal{B}_{\mathbf{k}}$, and $3\Lambda_q - \Lambda_p$ is positive definite for $\mathbf{k}\in\mathcal{B}_{\mathbf{k}}$, $\delta_x\neq\delta_y$ or $\delta_x\neq\delta_z$. Furthermore, the eigendecomposition of A is shown in the following theorem.

Theorem 7 (*Eigendecomposition of A [15]*)**.** *Let Λ_q, Λ_p, and T be defined in (31), (32) and (34), respectively. Also assume that $\mathbf{k}\in\mathcal{B}$. We have*

$$Q^*AQ = \mathrm{diag}\left(0, \Lambda_q, \Lambda_q\right). \tag{35}$$

Here,

$$Q = (I_3\otimes T)\begin{bmatrix}\Lambda_{\mathbf{x}} & \left(\Lambda_q - \Lambda_{\mathbf{x}}\Lambda_s^*\right) & \left(\Lambda_{\mathbf{z}}^* - \Lambda_{\mathbf{y}}^*\right)\\ \Lambda_{\mathbf{y}} & \left(\Lambda_q - \Lambda_{\mathbf{y}}\Lambda_s^*\right) & \left(\Lambda_{\mathbf{x}}^* - \Lambda_{\mathbf{z}}^*\right)\\ \Lambda_{\mathbf{z}} & \left(\Lambda_q - \Lambda_{\mathbf{z}}\Lambda_s^*\right) & \left(\Lambda_{\mathbf{y}}^* - \Lambda_{\mathbf{x}}^*\right)\end{bmatrix}$$
$$\mathrm{diag}\left(\Lambda_q^{-\frac{1}{2}}, \left(3\Lambda_q^2 - \Lambda_q\Lambda_p\right)^{-\frac{1}{2}}, \left(3\Lambda_q - \Lambda_p\right)^{-\frac{1}{2}}\right). \tag{36}$$

and Q is unitary.

The eigendecomposition stated in Theorem 7 is actually a powerful tool to reduce the $3n \times 3n$ GEVP (29) to another $2n \times 2n$ standard eigenvalue problem (SEVP) that both of the GEVP and SEVP have the same *nonzero* $2n$ eigenvalues. In other words, this SEVP excludes the n zero eigenvalues in the GEVP [15]. The inverse Lanczos method [19] thus becomes an efficient eigenvalue solver to compute the smallest positive eigenvalues of the SEVP that are of interest. In contrast, for the GEVP, the target smallest positive eigenvalues are located in the interior of the eigenvalue spectrum. The convergence behaviors of the shift-invert Lanczos method and the Jacobi–Davidson method are significantly affected by the n zero eigenvalues [20]. In short, the SEVP not only has smaller size, the eigenvalue solver can converge faster [15].

Now, we describe how the $2n \times 2n$ SEVP can be derived from Theorem 7. More details can be found in [15]. Eq. (35) suggests that

$$A = Q^* \begin{bmatrix} 0 & \Lambda_q & \\ & & \Lambda_q \end{bmatrix} Q = (I_3 \otimes T)\, \Lambda \begin{bmatrix} \Lambda_q & \\ & \Lambda_q \end{bmatrix} \Lambda^* \left(I_3 \otimes T^*\right), \tag{37}$$

where

$$\Lambda = \begin{bmatrix} \left(\Lambda_q - \Lambda_{\mathbf{x}}\Lambda_s^*\right)\left(3\Lambda_q^2 - \Lambda_q\Lambda_p\right)^{-\frac{1}{2}} & \left(\Lambda_{\mathbf{z}}^* - \Lambda_{\mathbf{y}}^*\right)\left(3\Lambda_q - \Lambda_p\right)^{-\frac{1}{2}} \\ \left(\Lambda_q - \Lambda_{\mathbf{y}}\Lambda_s^*\right)\left(3\Lambda_q^2 - \Lambda_q\Lambda_p\right)^{-\frac{1}{2}} & \left(\Lambda_{\mathbf{x}}^* - \Lambda_{\mathbf{z}}^*\right)\left(3\Lambda_q - \Lambda_p\right)^{-\frac{1}{2}} \\ \left(\Lambda_q - \Lambda_{\mathbf{z}}\Lambda_s^*\right)\left(3\Lambda_q^2 - \Lambda_q\Lambda_p\right)^{-\frac{1}{2}} & \left(\Lambda_{\mathbf{y}}^* - \Lambda_{\mathbf{x}}^*\right)\left(3\Lambda_q - \Lambda_p\right)^{-\frac{1}{2}} \end{bmatrix}. \tag{38}$$

Letting A_s be a 3×2 block matrix that

$$A_s = (I_3 \otimes T)\, \Lambda \mathrm{diag}\left(\Lambda_q^{\frac{1}{2}}, \Lambda_q^{\frac{1}{2}}\right), \tag{39}$$

we can rewrite Eq. (37) as $A = A_s A_s^*$ and then we have the following theorem.

Theorem 8. *Let A and A_s be defined in (30) and (39), respectively, and $\mathbf{k} \in \mathcal{B}$. Then*

$$\mathrm{span}\left\{B^{-1}A_s\right\} = \{\mathbf{e};\, A\mathbf{e} = \lambda B\mathbf{e},\ \lambda > 0\}.$$

From the result in Theorem 8, we take

$$\mathbf{e} = B^{-1}A_s\mathbf{e}_r. \tag{40}$$

Substituting $\mathbf{e}$ in (40) into (29) and using the fact that $A = A_sA_s^*$, the GEVP (29) becomes

$$\left(A_sA_s^*\right)\left(B^{-1}A_s\mathbf{e}_r\right) = \lambda A_s\mathbf{e}_r. \tag{41}$$

Pre-multiplying (41) by A_s^* and using the non-singularity of $A_s^*A_s$, we can form the following SEVP

$$\left(A_s^*B^{-1}A_s\right)\mathbf{e}_r = \lambda\mathbf{e}_r. \tag{42}$$

It is clear that the coefficient matrix $\left(A_s^*B^{-1}A_s\right)$ of the above SEVP is a 2×2 block matrix. Finally, the inverse Lanczos method is applied to compute a few smallest positive eigenvalues of (42) that are of interest, as all of the eigenvalues in the SEVP are positive.

We summarize the inverse projective Lanczos method (IPL) [15] for solving GEVP (29) via the SEVP (42) in Algorithm 1. More details of the fast algorithms within the IPL can be found in [15].

Algorithm 1 Inverse projective Lanczos method for solving (29)

1: Compute $\Lambda_{\mathbf{x}}$, $\Lambda_{\mathbf{y}}$, and $\Lambda_{\mathbf{z}}$ in (33);
2: Compute Λ_q, Λ_p, and Λ_s in (31) and (32), respectively;
3: Compute Λ as defined in Eq. (38).
4: Apply the inverse Lanczos method to solve the SEVP in (42);
5: Compute $\mathbf{e}$ by Eq. (40).

5. Numerical results

The eigenvalue solver due to the explicit matrix representation described in Section 3 are carried out by using MATLAB 2011b. All numerical computations are performed on a HP workstation with two Intel Quad-Core Xeon X5687 3.6 GHz

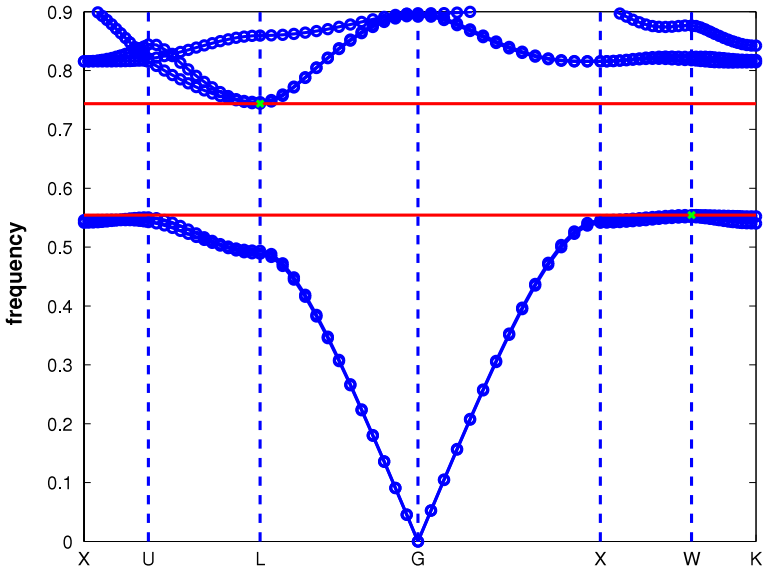

Fig. 1. Band structure of the 3D photonic crystals with FCC lattice. The vectors **k**'s along the boundary of first Brillouin zone. The frequency $\omega = a\sqrt{\lambda}/(2\pi)$ is shown on the y-axis. The radius of the sphere is $r = 0.12a$ and the connecting spheroid has minor axis length $s = 0.09a$. In the figure, the notation G means Γ.

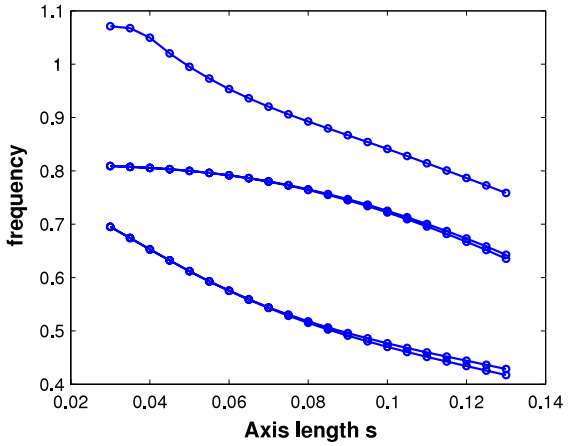

(a) Fixed $r = 0.12$.

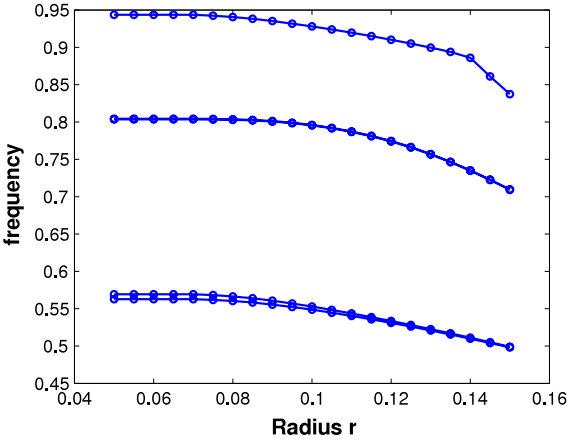

(b) Fixed $s = 0.07$.

Fig. 2. The five smallest frequencies with various s and r for $n = 1{,}728{,}000$.

CPUs, 48 GB main memory, and RedHat Linux operation system. The IEEE double-precision floating-point arithmetic is used. For the geometric structure regarding the 3D photonic crystal with FCC lattice, we consider the structure that consists of dielectric spheres with connecting spheroid [2]. The radius r of the spheres and the minor axis length s of the spheroid are $r/a = 0.12$ and $s/a = 0.09$, respectively. Inside the structure is the dielectric material with permittivity contrast $\varepsilon_i/\varepsilon_o = 13$.

First, we solve the eigenvalue problems associated with the **k**'s along the segments connecting X, U, L, Γ, X, W, and K. In each of the segments, fifteen uniform distributed sampling vectors **k** are chosen. The number of grid points $n_1 = 24$, $n_2 = 24$, and $n_3 = 24$. The size of A is $41{,}472 \times 41{,}472$. Fig. 1 shows the computed band structure of the 3D photonic crystals with FCC lattice versus the sampling vectors **k**. Clearly, a band gap lies between the second and third smallest positive eigenvalues.

Second, we conduct numerical experiments to evaluate performances of the IPL eigenvalue solver described in Section 4 for solving the GEVP (29) with various geometric parameters r and s. In each set of r and s parameter combinations, we consider the **k** vector located in the corner L of the irreducible Brillouin zone and compute the five smallest positive eigenvalues with $n_1 = n_2 = n_3 = 120$. The size of A is $5{,}184{,}000 \times 5{,}184{,}000$. In the first test problem set, $r = 0.12$ and s ranges from 0.03 to 0.13. In the second test problem set, $s = 0.07$ and r ranges from 0.05 to 0.15. The computed frequencies are shown in Fig. 2. The corresponding CPU time and iteration numbers of the IPL method are shown in Figs. 3 and 4 for the first and second test problem set, respectively. These results show that the eigenvalue solver based on the IPL method

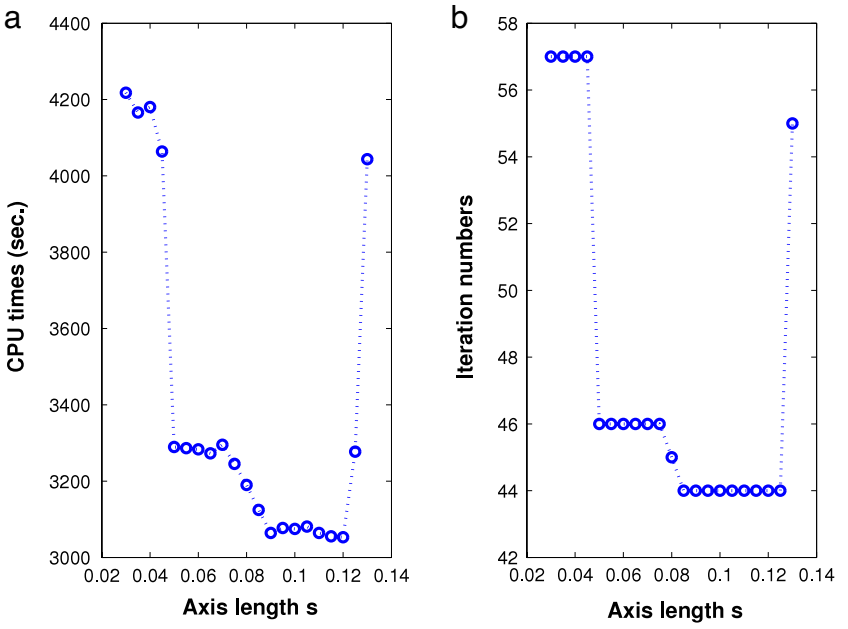

Fig. 3. CPU time and iteration numbers of the IPL eigenvalue solver. The radius r of the spheres is fixed to 0.12 and the minor axis length s is shown on the x-axis of the figures.

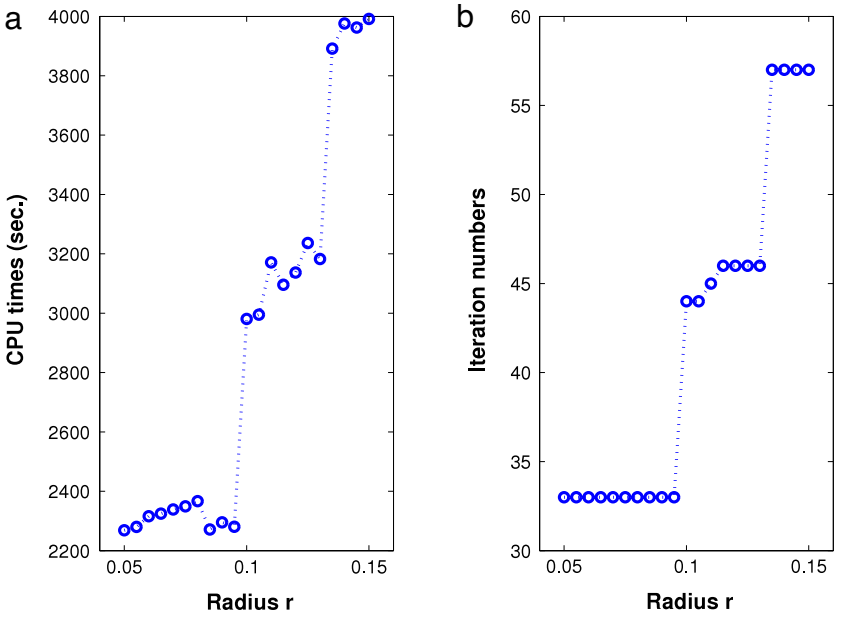

Fig. 4. CPU time and iteration numbers of the IPL eigenvalue solver. The minor axis length s of the spheroid is fixed to 0.07. The radius r of the spheres is shown on the x-axis of the figures.

is both robust and efficient with respect to different r and s. The IPL eigenvalue solver successfully finds all the band-gap corresponding to the various photonic structures. The solver is quite fast. Out of all of the 42 test problems whose dimension are as large as 3.5 millions ($2n_1^3$), the IPL eigenvalue solver takes only 38–70 min (with average of 53 min) to solve each of the eigenvalue problems. It is also worth mentioning that the iteration numbers are small for such large eigenvalue problems.

6. Conclusion

An explicit matrix representation for the three-dimensional face centered cubic photonic crystal is described for the first time. The matrix is constructed by applying Yee's scheme to discretize the governing Maxwell equations. The matrix

representation benefits the computations significantly by leading to (i) the eigendecomposition of the degenerate coefficient matrix corresponding to the discrete double-curl operator with the Maxwell equations and (ii) an efficient inverse projective Lanczos method based eigenvalue solver. Numerical results show that the eigenvalue solver is robust and efficient for various geometric structure of the photonic crystals. All of these results form a useful tool to conduct photonic crystal shape optimization for the largest possible band-gap. A reasonable, yet non-trivial, future direction is to generalize the results to other lattice structures like simple cubic lattice and body centered cubic lattice.

Acknowledgments

This work is partially supported by the National Science Council, the Taida Institute of Mathematical Sciences, the Center for Advanced Study in Theoretical Sciences, and the National Center for Theoretical Sciences in Taiwan.

Appendix

Proof of Theorem 4. By the periodic condition (2), we have

$$\begin{aligned}
&E_1(\widehat{-1}, j, k) = e^{-\imath 2\pi \mathbf{k}\cdot\mathbf{a}_1} E_1(\hat{n}_1 - 1, j, k),\\
&E_3(0, j, \hat{k}) = e^{-\imath 2\pi \mathbf{k}\cdot\mathbf{a}_1} E_3(n_1, j, \hat{k}), \quad \text{and}\\
&E_3(-1, j, \hat{k}) = e^{-\imath 2\pi \mathbf{k}\cdot\mathbf{a}_1} E_3(n_1 - 1, j, \hat{k}).
\end{aligned}$$

From (22b), we have

$$\begin{aligned}
H_2(\widehat{-1}, j, \hat{k}) &= e^{-\imath 2\pi \mathbf{k}\cdot\mathbf{a}_1}\left(\frac{E_1(\hat{n}_1 - 1, j, k+1) - E_1(\hat{n}_1 - 1, j, k)}{\delta_z} - \frac{E_3(n_1, j, \hat{k}) - E_3(n_1 - 1, j, \hat{k})}{\delta_x}\right)\\
&= e^{-\imath 2\pi \mathbf{k}\cdot\mathbf{a}_1} H_2(\hat{n}_1 - 1, j, \hat{k}).
\end{aligned}$$

Similarly, it holds that $H_3(\widehat{-1}, \hat{j}, k) = e^{-\imath 2\pi \mathbf{k}\cdot\mathbf{a}_1} H_3(\hat{n}_1 - 1, \hat{j}, k)$. □

Proof of Theorem 5. Observing

$$\mathbf{x}(i, \widehat{-1}, k) = -\mathbf{a}_2 + \left(\frac{3m_1 + i}{6m_1}\frac{a}{\sqrt{2}}, \left(6m_2 - \frac{1}{2}\right)\frac{1}{6m_2}\frac{a\sqrt{3}}{2\sqrt{2}}, k\delta_z\right),$$

we can see the following results. If $0 \le i < 3m_1$, then

$$\mathbf{x}(i, \widehat{-1}, k) = -\mathbf{a}_2 + \mathbf{x}(3m_1 + i, \hat{n}_2 - 1, k).$$

In other cases, i.e., $3m_1 \le i < 6m_1$,

$$\begin{aligned}
\mathbf{x}(i, \widehat{-1}, k) &= -\mathbf{a}_2 + \mathbf{a}_1 + \left(\frac{i - 3m_1}{6m_1}\frac{a}{\sqrt{2}}, \left(6m_2 - \frac{1}{2}\right)\frac{1}{6m_2}\frac{a\sqrt{3}}{2\sqrt{2}}, k\delta_z\right)\\
&= -\mathbf{a}_2 + \mathbf{a}_1 + \mathbf{x}(i - 3m_1, \hat{n}_2 - 1, k).
\end{aligned}$$

The above results suggest that

$$E_2(i, \widehat{-1}, k) = \begin{cases} e^{-\imath 2\pi \mathbf{k}\cdot\mathbf{a}_2} E_2(3m_1 + i, \hat{n}_2 - 1, k), & \text{if } 0 \le i < 3m_1,\\ e^{-\imath 2\pi \mathbf{k}\cdot(\mathbf{a}_2 - \mathbf{a}_1)} E_2(i - 3m_1, \hat{n}_2 - 1, k), & \text{if } 3m_1 \le i < 6m_1. \end{cases} \tag{43}$$

Similarly, we also have

$$E_3(i, -\ell, \hat{k}) = \begin{cases} e^{-\imath 2\pi \mathbf{k}\cdot\mathbf{a}_2} E_3(3m_1 + i, n_2 - \ell, \hat{k}), & \text{if } 0 \le i < 3m_1,\\ e^{-\imath 2\pi \mathbf{k}\cdot(\mathbf{a}_2 - \mathbf{a}_1)} E_3(i - 3m_1, n_2 - \ell, \hat{k}), & \text{if } 3m_1 \le i < 6m_1, \end{cases} \tag{44}$$

for $\ell = 0, 1$. Using (22a) with $j = -1$ and the results in (43) and (44), we have the following results. If $0 \le i < 3m_1$, then

$$\begin{aligned}
H_1(i, \widehat{-1}, \hat{k}) &= e^{-\imath 2\pi \mathbf{k}\cdot\mathbf{a}_2}\left(\frac{E_3(3m_1 + i, n_2, \hat{k}) - E_3(3m_1 + i, n_2 - 1, \hat{k})}{\delta_y}\right)\\
&\quad - e^{-\imath 2\pi \mathbf{k}\cdot\mathbf{a}_2}\left(\frac{E_2(3m_1 + i, \hat{n}_2 - 1, k+1) - E_2(3m_1 + i, \hat{n}_2 - 1, k)}{\delta_z}\right)\\
&= e^{-\imath 2\pi \mathbf{k}\cdot\mathbf{a}_2} H_1(3m_1 + i, \hat{n}_2 - 1, \hat{k}).
\end{aligned}$$

If $3m_1 \le i < 6m_1$, then

$$\begin{aligned} H_1(i, \widehat{-1}, \hat{k}) &= e^{-\imath 2\pi \mathbf{k}\cdot(\mathbf{a}_2-\mathbf{a}_1)} \left(\frac{E_3(i-3m_1, n_2, \hat{k}) - E_3(i-3m_1, n_2-1, \hat{k})}{\delta_y} \right) \\ &\quad - e^{-\imath 2\pi \mathbf{k}\cdot(\mathbf{a}_2-\mathbf{a}_1)} \left(\frac{E_2(i-3m_1, \hat{n}_2-1, k+1) - E_2(i-3m_1, \hat{n}_2-1, k)}{\delta_z} \right) \\ &= e^{-\imath 2\pi \mathbf{k}\cdot(\mathbf{a}_2-\mathbf{a}_1)} H_1(i-3m_1, \hat{n}_2-1, \hat{k}). \end{aligned}$$

The aforementioned results suggest that

$$H_1(0 : n_1-1, \widehat{-1}, \hat{k}) = e^{-\imath 2\pi \mathbf{k}\cdot\mathbf{a}_2} J_2^* H_1(0 : n_1-1, \hat{n}_2-1, \hat{k}).$$

Finally, by using the same technique, we can show that

$$H_3(\hat{0} : \hat{n}_1-1, \widehat{-1}, k) = e^{-\imath 2\pi \mathbf{k}\cdot\mathbf{a}_2} J_2^* H_3(\hat{0} : \hat{n}_1-1, \hat{n}_2-1, k). \quad \square$$

Proof of Theorem 6. By the fact

$$\mathbf{x}(i, \hat{j}, -1) = -\mathbf{a}_3 + \left(\frac{i+3m_1}{6m_1}\frac{a}{\sqrt{2}}, \frac{j+1/2+2m_2}{6m_2}\frac{a\sqrt{3}}{2\sqrt{2}}, \frac{n_3-1}{n_3}\frac{a}{\sqrt{3}} \right),$$

we have the following results. If $0 \le j < 4m_2$ and $0 \le i < 3m_1$, then

$$\mathbf{x}(i, \hat{j}, -1) = -\mathbf{a}_3 + \mathbf{x}(i+3m_1, \hat{j}+2m_2, n_3-1).$$

If $0 \le j < 4m_2$ and $3m_1 \le i < 6m_1$, then

$$\begin{aligned} \mathbf{x}(i, \hat{j}, -1) &= -\mathbf{a}_3 + \mathbf{a}_1 + \left(\frac{i-3m_1}{6m_1}\frac{a}{\sqrt{2}}, \frac{j+1/2+2m_2}{6m_2}\frac{a\sqrt{3}}{2\sqrt{2}}, \frac{n_3-1}{n_3}\frac{a}{\sqrt{3}} \right) \\ &= -\mathbf{a}_3 + \mathbf{a}_1 + \mathbf{x}(i-3m_1, \hat{j}+2m_2, n_3-1). \end{aligned}$$

Otherwise, i.e., $4m_2 \le j < 6m_2$, we have

$$\begin{aligned} \mathbf{x}(i, \hat{j}, -1) &= -\mathbf{a}_3 + \mathbf{a}_2 + \left(\frac{i}{6m_1}\frac{a}{\sqrt{2}}, \frac{j+1/2-4m_2}{6m_2}\frac{a\sqrt{3}}{2\sqrt{2}}, \frac{n_3-1}{n_3}\frac{a}{\sqrt{3}} \right) \\ &= -\mathbf{a}_3 + \mathbf{a}_2 + \mathbf{x}(i, \hat{j}-4m_2, n_3-1). \end{aligned}$$

Consequently, by the periodic condition in (2), $E_2(i, \hat{j}, -1)$ can be rewritten as

$$E_2(i, \hat{j}, -1) = \begin{cases} e^{-\imath 2\pi \mathbf{k}\cdot\mathbf{a}_3} E_2(i+3m_1, \hat{j}+2m_2, n_3-1), & \text{if } 0 \le j < 4m_2,\ 0 \le i < 3m_1, \\ e^{\imath 2\pi \mathbf{k}\cdot(\mathbf{a}_1-\mathbf{a}_3)} E_2(i-3m_1, \hat{j}+2m_2, n_3-1), & \text{if } 0 \le j < 4m_2,\ 3m_1 \le i < 6m_1, \\ e^{\imath 2\pi \mathbf{k}\cdot(\mathbf{a}_2-\mathbf{a}_3)} E_2(i, \hat{j}-4m_2, n_3-1), & \text{if } 4m_2 \le j < 6m_2. \end{cases} \tag{45a}$$

Similarly, we also have

$$E_3(i, j, \widehat{-1}) = \begin{cases} e^{-\imath 2\pi \mathbf{k}\cdot\mathbf{a}_3} E_3(i+3m_1, j+2m_2, \hat{n}_3-1), & \text{if } 0 \le j < 4m_2,\ 0 \le i < 3m_1, \\ e^{\imath 2\pi \mathbf{k}\cdot(\mathbf{a}_1-\mathbf{a}_3)} E_3(i-3m_1, j+2m_2, \hat{n}_3-1), & \text{if } 0 \le j < 4m_2,\ 3m_1 \le i < 6m_1, \\ e^{\imath 2\pi \mathbf{k}\cdot(\mathbf{a}_2-\mathbf{a}_3)} E_3(i, j-4m_2, \hat{n}_3-1), & \text{if } 4m_2 \le j < 6m_2. \end{cases} \tag{45b}$$

Using (22a) with $k = -1$ and the results in (45), we obtain the following results. If $0 \le j < 4m_2$ and $0 \le i < 3m_1$, then

$$\begin{aligned} H_1(i, \hat{j}, \widehat{-1}) &= e^{-\imath 2\pi \mathbf{k}\cdot\mathbf{a}_3} \left(\frac{E_3(i+3m_1, j+2m_2+1, \hat{n}_3-1) - E_3(i+3m_1, j+2m_2, \hat{n}_3-1)}{\delta_y} \right) \\ &\quad - e^{-\imath 2\pi \mathbf{k}\cdot\mathbf{a}_3} \left(\frac{E_2(i+3m_1, \hat{j}+2m_2, n_3) - E_2(i+3m_1, \hat{j}+2m_2, n_3-1)}{\delta_z} \right) \\ &= e^{-\imath 2\pi \mathbf{k}\cdot\mathbf{a}_3} H_1(i+3m_1, \hat{j}+2m_2, \hat{n}_3-1). \end{aligned}$$

That is,

$$H_1(0 : 3m_1-1, \hat{0} : \widehat{4m_2}-1, \widehat{-1}) = e^{-\imath 2\pi \mathbf{k}\cdot\mathbf{a}_3} H_1(3m_1 : 6m_1-1, \widehat{2m_2} : \widehat{6m_2}-1, \hat{n}_3-1). \tag{46}$$

If $0 \le j < 4m_2$ and $3m_1 \le i < 6m_1$, then

$$\begin{aligned} H_1(i,\hat{j},\widehat{-1}) &= e^{\imath 2\pi \mathbf{k}\cdot(\mathbf{a}_1-\mathbf{a}_3)}\left(\frac{E_3(i-3m_1, j+2m_2+1, \hat{n}_3-1) - E_3(i-3m_1, j+2m_2, \hat{n}_3-1)}{\delta_y}\right) \\ &\quad - e^{\imath 2\pi \mathbf{k}\cdot(\mathbf{a}_1-\mathbf{a}_3)}\left(\frac{E_2(i-3m_1, \hat{j}+2m_2, n_3) - E_2(i-3m_1, \hat{j}+2m_2, n_3-1)}{\delta_z}\right) \\ &= e^{\imath 2\pi \mathbf{k}\cdot(\mathbf{a}_1-\mathbf{a}_3)} H_1(i-3m_1, \hat{j}+2m_2, \hat{n}_3-1). \end{aligned}$$

That is,

$$H_1(3m_1 : 6m_1-1, \hat{0} : \widehat{4m_2}-1, \widehat{-1}) = e^{\imath 2\pi \mathbf{k}\cdot(\mathbf{a}_1-\mathbf{a}_3)} H_1(0 : 3m_1-1, \widehat{2m_2} : \widehat{6m_2}-1, \hat{n}_3-1). \tag{47}$$

In other cases, i.e., $4m_2 \le j < 6m_2$, we have

$$\begin{aligned} H_1(i,\hat{j},\widehat{-1}) &= e^{\imath 2\pi \mathbf{k}\cdot(\mathbf{a}_2-\mathbf{a}_3)}\left(\frac{E_3(i, j-4m_2+1, \hat{n}_3-1) - E_3(i, j-4m_2, \hat{n}_3-1)}{\delta_y}\right) \\ &\quad - e^{\imath 2\pi \mathbf{k}\cdot(\mathbf{a}_2-\mathbf{a}_3)}\left(\frac{E_2(i, \hat{j}-4m_2, n_3) - E_2(i, \hat{j}-4m_2, n_3-1)}{\delta_z}\right) \\ &= e^{\imath 2\pi \mathbf{k}\cdot(\mathbf{a}_2-\mathbf{a}_3)} H_1(i, \hat{j}-4m_2, \hat{n}_3-1). \end{aligned}$$

That is,

$$H_1(0 : 6m_1-1, \widehat{4m_2} : \widehat{6m_2}-1, \widehat{-1}) = e^{\imath 2\pi \mathbf{k}\cdot(\mathbf{a}_2-\mathbf{a}_3)} H_1(0 : 6m_1-1, \hat{0} : \widehat{2m_2}-1, \hat{n}_3-1). \tag{48}$$

Combining the results in (46)–(48), we obtain the periodicity shown in (26). The periodicity shown in (27) can be proved similarly. □

References

[1] A. Chatterjee, J.M. Jin, J.L. Volakis, Computation of cavity resonances using edge-based finite elements, IEEE Trans. Microw. Theory Tech. 40 (1992) 2106–2108.
[2] R.L. Chern, C. Chung Chang, Chien-C. Chang, R.R. Hwang, Numerical study of three-dimensional photonic crystals with large band gaps, J. Phys. Soc. Japan 73 (2004) 727–737.
[3] P. Arbenz, A comparison of factorization-free eigensolvers with application to cavity resonators, in: Lecture Notes in Computer Science, Springer, Berlin, 2009.
[4] P. Arbenz, R. Geus, A comparison of solvers for large eigenvalue problems occuring in the design of resonant cavities, Numer. Linear Algebra Appl. 6 (1999) 3–16.
[5] P. Arbenz, R. Geus, Multilevel preconditioned iterative eigensolvers for Maxwell eigenvalue problems, Appl. Numer. Math. 54 (2) (2005) 107–121.
[6] Z. Bai, J. Demmel, J. Dongarra, A. Ruhe, H. van der Vorst, Templates for the Solution of Algebraic Eigenvalue Problems: A Practical Guide, SIAM, Philadelphia, 2000.
[7] D.R. Fokkema, G.L.G. Sleijpen, H.A. van der Vorst, Jacobi–Davidson style QR and QZ algorithms for the reduction of matrix pencils, SIAM J. Sci. Comput. 20 (1998) 94–125.
[8] T.-M. Huang, W.-J. Chang, Y.-L. Huang, W.-W. Lin, W.-C. Wang, W. Wang, Preconditioning bandgap eigenvalue problems in three dimensional photonic crystals simulations, J. Comput. Phys. 229 (2010) 8684–8703.
[9] T.-M. Huang, Y.-L. Huang, W.-W. Lin, W.-C. Wang, A null space free Jacobi–Davidson iteration for Maxwells operator, Technical Report, NCTS Preprints in Mathematics, National Tsing Hua University, Hsinchu, Taiwan, 2009-7-004, 2009.
[10] G.L.G. Sleijpen, A.G.L. Booten, D.R. Fokkema, H.A. van der Vorst, Jacobi–Davidson type methods for generalized eigenproblems and polynomial eigenproblems, BIT 36 (1996) 595–633.
[11] G.L.G. Sleijpen, H.A. van der Vorst, A Jacobi–Davidson iteration method for linear eigenvalue problems, SIAM J. Matrix Anal. Appl. 17 (1996) 401–425.
[12] R.L. Chern, C. Chung Chang, Chien-C. Chang, R.R. Hwang, Large full band gaps for photonic crystals in two dimensions computed by an inverse method with multgrid acceleration, Phys. Rev. E 68 (2003) 26704.
[13] R. Hiptmair, K. Neymeyr, Multilevel method for mixed eigenproblems, SIAM J. Sci. Comput. 23 (2002) 2141–2164.
[14] V. Simoncini, Algebraic formulations for the solution of the nullspace-free eigenvalue problem using the inexact shift-and-invert Lanczos method, Numer. Linear Algebra Appl. 10 (2003) 357–375.
[15] T.-M. Huang, H.-E. Hsieh, W.-W. Lin, W. Wang, Eigendecomposition of the discrete double-curl operator with application to fast eigensolver for three dimensional photonic crystals, Technical Report, National Center for Theoretical Sciences, 2012.
[16] C. Kittel, Introduction to Solid State Physics, Wiley, New York, 2005.
[17] K. Yee, Numerical solution of initial boundary value problems involving Maxwell's equations in isotropic media, IEEE Trans. Antennas and Propagation 14 (1966) 302–307.
[18] J.D. Joannopoulos, S.G. Johnson, J.N. Winn, R.D. Meade, Photonic Crystals: Molding the Flow of Light, Princeton University Press, 2008.
[19] G.H. Golub, C.F. Van Loan, Matrix Computations, third ed., The Johns Hopkins University Press, 1996.
[20] T.-M. Huang, Y.-C. Kuo, W. Wang, Computing spectrum boundary eigenvalues for three-dimensional photonic crystals, 2012. Preprint.